Atmospheric Environment 147 (2016) 88–97

Contents lists available at ScienceDirect

Atmospheric Environment

journal homepage: www.elsevier.com/locate/atmosenv

Assessing the role of soil water limitation in determining the Phytotoxic Ozone Dose (PODY) thresholds

Alessandra De Marco [a, *], Pierre Sicard [b], Silvano Fares [c], Juha-Pekka Tuovinen [d], Alessandro Anav [a], Elena Paoletti [e]

[a] ENEA, Casaccia, Rome, Italy
[b] ACRI-HE, Sophia Antipolis-Cedex, France
[c] CREA-RPS, Rome, Italy
[d] FMI, Helsinki, Finland
[e] CNR, Florence, Italy

HIGHLIGHTS

- The difference between the PODY with and without soil water limitation is not negligible.
- This difference significantly increases with increasing *Y* thresholds.
- This difference is higher for Mediterranean vegetation than for temperate vegetation.

ARTICLE INFO

Article history:
Received 11 March 2016
Received in revised form
6 September 2016
Accepted 28 September 2016
Available online 28 September 2016

Keywords:
DO_3SE model
Ozone risk assessment
Phytotoxic Ozone Dose
Soil water content
Threshold
Mediterranean forests

ABSTRACT

Phytotoxic Ozone Dose (PODY), defined as the accumulated stomatal ozone flux over a threshold of *Y*, is considered an optimal metric to evaluate O_3 effects on vegetation. PODY is often computed through the DO_3SE model, which includes species-specific parameterizations for the environmental response of stomatal conductance. However, the effect of soil water content (SWC) on stomatal aperture is difficult to model on a regional scale and thus often ignored. In this study, we used environmental input data obtained from the WRF-CHIMERE model for 14,546 grid-based forest sites in Southern Europe. SWC was obtained for the upper 10 cm of soil, which resulted in a worst-case risk scenario. PODY was calculated either with or without water limitation for different *Y* thresholds. Exclusion of the SWC effect on stomatal fluxes caused a serious overestimation of PODY. The difference increased with increasing *Y* (78%, 128%, 237% and 565% with $Y = 0, 1, 2$ and 3 nmol O_3 m^{-2} s^{-1}, respectively). This behaviour was confirmed by applying the same approach to field data measured in a Mediterranean *Quercus ilex* forest. WRF-CHIMERE overestimated SWC at this field site, so under real-world conditions the SWC effect may be larger than modelled. The differences were lower for temperate species (*Pinus cembra* 50–340%, *P. sylvestris* 57–363%, *Abies alba* 57–371%) than for Mediterranean species (*P. pinaster* 87–356%, *P. halepensis* 96–429%, *P. pinea* 107–532%, *Q. suber* 104–1602%), although a high difference was recorded also for the temperate species *Fagus sylvatica* with POD3 (524%). We conclude that SWC should be considered in PODY simulations and a low *Y* threshold should be used for robustness.

1. Introduction

Ozone (O_3) is a key air pollutant and a powerful greenhouse gas (IPCC, 2014). In the Northern hemisphere, tropospheric concentrations have approximately doubled in the last century (Vingarzan, 2004). Emission control measures have successfully reduced the peaks, while annual averages are still increasing (Sicard et al., 2013, 2016a; Paoletti et al., 2014). Intense solar radiation, high air temperature and stagnation of the air promote O_3 formation from its precursors, i.e. nitrogen oxides, volatile organic compounds, carbon monoxide and methane (e.g. Fiore et al., 2002; Sicard et al., 2009).

* Corresponding author.
E-mail addresses: alessandra.demarco@enea.it (A. De Marco), pierre.sicard@acri-he.fr (P. Sicard), silvano.fares@crea.gov.it (S. Fares), juha-pekka.tuovinen@fmi.fi (J.-P. Tuovinen), elena.paoletti@cnr.it (E. Paoletti).

http://dx.doi.org/10.1016/j.atmosenv.2016.09.066
1352-2310/

This is why O_3 concentrations are more elevated in Southern European countries bordering the Mediterranean sea, where photochemical activity is strong (Butkovic et al., 1990), than in central and Northern Europe (EEA, 2013). Ozone is considered a serious phytotoxic threat to all vegetation (Paoletti, 2007), and present tropospheric concentrations are high enough to negatively affect terrestrial ecosystems (Wittig et al., 2009; Mills et al., 2011a: Fares et al., 2013a). Even though Mediterranean vegetation is adapted to face oxidative stressors, such as water deficit, heat and elevated solar radiation, and is thus more O_3 tolerant than mesophilic vegetation (Paoletti, 2006), visible O_3-induced foliar injury occurs (Günthardt-Goerg and Vollenweider, 2007; Paoletti et al., 2009a,b; Sicard et al., 2010; Mills et al., 2011a; Sicard et al., 2016b), suggesting that atmospheric concentrations of O_3 reach toxic levels.

In the last decades, scientific consensus has been reached to recommend the use of stomatal O_3 flux to evaluate O_3 effects on vegetation, as it can explain the observed effects better than ambient O_3 concentration (Paoletti and Manning, 2007; Mills et al., 2011b). Ozone uptake through stomata can be calculated using the multiplicative model of stomatal conductance (Jarvis, 1976), introduced within the risk assessment methodology of the UNECE Convention on Long-range Transboundary Air Pollution (CLRTAP) as the Deposition of Ozone for Stomatal Exchange (DO$_3$SE) model (Emberson et al., 2000, 2001; CLRTAP, 2015). By introducing a threshold flux (*Y*) to reflect detoxification processes, and by accumulating over the growing season, we obtain the Phytotoxic Ozone Dose (POD*Y*), a flux-based impact index that incorporates the effects of plant phenology and the most important environmental variables on stomatal function, i.e. air temperature, solar radiation, vapour pressure deficit and soil water content (SWC). However, the scarcity of measured data and/or reliable soil moisture models has been a serious obstacle to the inclusion of stomatal SWC limitation in POD*Y* calculations, thus resulting in the compromise of considering 'worst-case' impact scenarios with no SWC effects on O_3 fluxes (Simpson et al., 2007; Tuovinen et al., 2009; CLRTAP, 2015). For example, SWC has been incorporated into the recent versions of the EMEP chemical transport model (Simpson et al., 2012), which is widely employed within the European air pollution abatement work; however, an explicit treatment of SWC effect is deliberately ignored in the POD*Y* calculations that serve scenario analysis and optimisation runs with large-scale integrated assessment models (CLRTAP, 2015). This kind of scenario is helpful when determining ozone risk for soils and regions that rarely experience drought stress, or when working with irrigated crops or irrigated trees, but is poorly applicable in risk assessment for unirrigated forests, especially in the Mediterranean region.

Different threshold fluxes, below which O_3 uptake is assumed to cause no injury to plants, are assumed for different vegetation types (CLRTAP, 2015; Mills et al., 2011a). At present, a threshold $Y = 1$ nmol O_3 m^{-2} s^{-1} (i.e. POD1) is recommended for the protection of forests and grasslands (CLRTAP, 2015), $Y = 6$ nmol O_3 m^{-2} s^{-1} is recommended for crops (CLRTAP, 2015), and a value of $Y = 2$ nmol O_3 m^{-2} s^{-1} is under discussion as a potentially new threshold for forests (Büker et al., 2015).

By using modelled input data for grid-based forest sites distributed in temperate and Mediterranean climates in Southern Europe, we here aim at quantifying the differences resulting from using DO$_3$SE for the calculation of POD*Y* without considering water limitation to stomatal exchange, as compared to the full model. As the sensitivity of such a threshold-based index to changes in the input is known to increase with increasing threshold (Tuovinen et al., 2007), we also quantify how this difference depends on the threshold flux *Y*. This knowledge is needed for a proper modelling of global O_3 risks to vegetation and for selecting the best legislative standards to protect plants from O_3. We hypothesize that (i) the difference between the POD*Y* values calculated with and without soil water limitation is not negligible; (ii) this difference significantly increases with increasing *Y* thresholds; and (iii) this difference is higher for Mediterranean vegetation than for temperate vegetation. As the magnitude of these effects may be affected by the accuracy of the models employed, similar calculations were performed with field data measured at a Mediterranean forest site. The aim of this comparison with measured data was to confirm the magnitude of the differences, rather than to validate the model which would require much more field data.

2. Materials and methods

2.1. Study area and input data modelling

Hourly mean values of air temperature, relative humidity, SWC, solar radiation and O_3 concentration for 2012 and 2013 within our study region (Fig. 1) were obtained from the WRF-CHIMERE modelling system and used as input for the DO$_3$SE model for calculating the leaf-level stomatal fluxes and POD*Y* values. The model domain and settings of these calculations were similar to those adopted within a recent study by Anav et al. (2016). CHIMERE is a regional-scale chemical transport model that is designed to produce hourly data of O_3, aerosol and other pollutants (Bessagnet et al., 2004). CHIMERE is forced by the Weather Research and Forecasting (WRF) model (Skamarock et al., 2008; De Meij et al., 2009; Sicard et al., 2012). WRF is available as a limited-area, non-hydrostatic, terrain-following sigma-coordinate model, designed to simulate mesoscale atmospheric circulation. WRF also provided the soil type data for our study area.

The modelling system was constituted by a two-way nesting between a mother domain at a coarse resolution across Europe (18 km as spatial resolution) and the nested domain (6 km) (Fig. 1A). The nesting ratio was 3:1, meaning that the nest's input from the coarse mesh comes via its boundaries, while the feedback to the coarser mesh occurs over the nest interior. The nested domain included 14,546 grid-based forest sites in south-eastern France, Slovenia, and northern and central Italy (Fig. 1B). Each site corresponded to a 6 km × 6 km pixel in the WRF-CHIMERE modelling system. The forest species occurrence in each pixel was determined by means of the EUFORGEN vegetation data (http://www.euforgen.org/distribution_maps.html). We selected this geographic region since it includes both soil water limited areas (the Mediterranean part of the total area) and non-water limited areas. The selected area also includes the most representative Mediterranean and temperate tree species. The sites were attributed to either Mediterranean or temperate climate zone on the basis of the bioclimatic classification (Rivas-Martinez, 1995) and the ecological characteristics of the forest species (Table 1).

The advanced Land Surface-hydrology Model (LSM-Noah), integrated into WRF, estimates water and energy fluxes within the soil and at the land-atmosphere interface. A detailed description of LSM-Noah is given by Chen and Dudhia (2001). LSM-Noah consists of four soil layers, with depths of 10, 30, 60 and 100 cm. The volumetric SWC is calculated for every layer by using the Richards equation. Within this work, SWC at the 0–10 cm depth was adopted so as to represent worst-case conditions, as the surface layers easily dry out, and as most of the absorbing fine roots concentrate in the top soil layer (Vinceti et al., 1998). This depth was also selected for comparison with field measurements of SWC (see below). The good performance of the WRF/LSM-Noah system in simulating SWC has previously been shown by comparisons with *in-situ* soil moisture observations from southern France (Greve et al., 2013), and with standard meteorological measurements as well as satellite-based and *in-situ* soil moisture data from Eastern

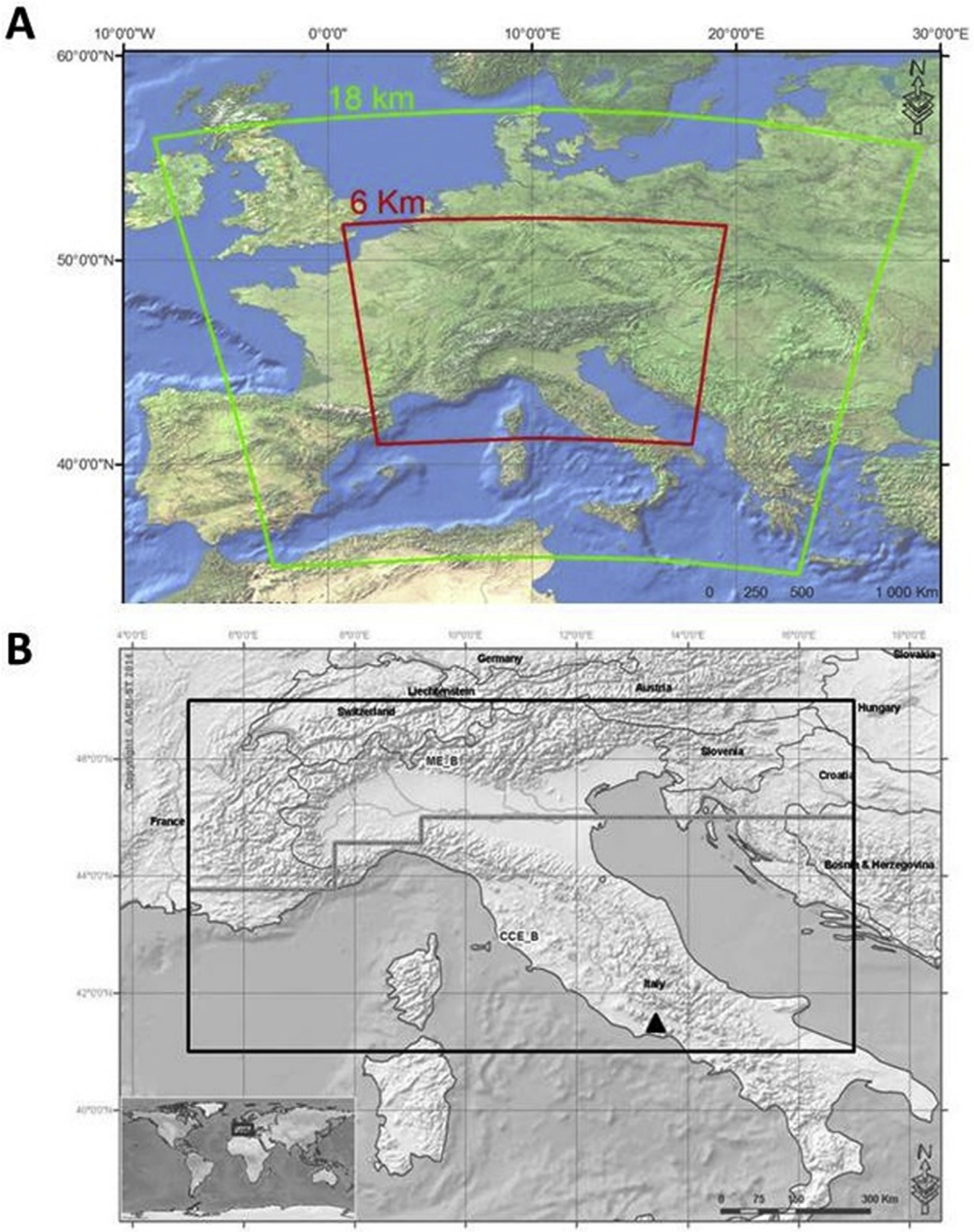

Fig. 1. Domains of the WRF-CHIMERE run (panel A). The green domain has a 18 km resolution and the red domain has a 6 km resolution. In panel B, the inner domain is shown with the regions adopted for the different CLRTAP (2015) parameterizations used for *Fagus sylvatica*, i.e. Continental Central Europe (CCE_B) and Mediterranean Europe (ME_B). The black triangle shows the location of the *Quercus ilex* forest at Castelporziano. (For interpretation of the references to colour in this figure legend, the reader is referred to the web version of this article.)

Texas (Kim and Nga, 2011). A good forecast skill of WRF with respect to SWC has also been demonstrated (e.g. Chen et al., 2007; Ceppi et al., 2013).

2.2. Phytotoxic Ozone Dose calculation

The stomatal conductance was calculated with the DO_3SE model, which is parameterized based on a large amount of measurement data and has been widely tested (Emberson et al., 2000, 2001, 2007; Tuovinen et al., 2001, 2004; Büker et al., 2007, 2012); presently DO_3SE constitutes the backbone of the CLRTAP risk assessment methodology mentioned above (CLRTAP, 2015). Hourly values of stomatal conductance of sunlit leaves at the top of the canopy, g_{sto}, expressed per projected leaf area, were calculated by

the following equation and the parameters shown in Tables 2 and 3:

$$g_{sto} = g_{max} \times f_{phen} \times f_{light} \times max\left(f_{min}, f_{temp} \times f_{VPD} \times f_{SWC}\right) \quad (1)$$

where g_{max} is the maximum stomatal conductance of a plant species and f_{min} is the minimum stomatal conductance expressed as a fraction of g_{max} (CLRTAP, 2015). The other terms are functions that represent the stomatal response to plant phenology and environmental conditions, expressed as scales from 0 to 1. f_{light}, f_{temp}, f_{VPD} and f_{SWC} describe the reduction of g_{sto} from g_{max} owing to suboptimal photosynthetic photon flux density, air temperature, vapour pressure deficit and volumetric SWC, respectively. In this study, the formulas obtained from CLRTAP (2015) were applied for f_{SWC}, f_{light}, f_{temp} and f_{VPD}.

SWC was estimated by the WRF model on the basis of soil type, with the data for different soil types obtained from LSM-Noah (Table 3). In the Mediterranean area, the functions of SWC and phenology are considered partly redundant, because the availability of water in the soil tracks the phenological development (CLRTAP, 2015, but see also Alonso et al., 2008). In our reference calculations, we included the f_{SWC} function and assumed that $f_{phen} = 1$ throughout the growing season. We used SWC rather than Soil Water Potential (SWP) because the availability of SWP data in the field is very limited and the modelling of SWP is challenging at a large scale.

We used the g_{sto} parameterizations available (Table 2) for Continental Central Europe (CCE) and Mediterranean Europe (ME) (CLRTAP, 2015). For the ME oak and ME and CCE beech, the lower limit of the g_{max} data summarized by CLRTAP (2015) was chosen (Di Matteo et al., 2014; Llusia et al., 2016), while for CCE Norway spruce the median value was considered more appropriate for the investigated area. As species- and region-specific flux parameterizations have only been derived for a few representative species, while our forest data identify nine different species, CCE Norway spruce was used for the temperate conifers *Pinus cembra, P. sylvestris* and *Abies alba;* ME *Quercus ilex* for the Mediterranean evergreen broadleaf species *Q. ilex* and *Q. suber;* and ME *P. halepensis* for the Mediterranean pines *P. halepensis, P. pinaster* and *P. pinea. Fagus sylvatica,* or European beech, is a deciduous broadleaf tree, whose natural range extends from southern Sweden to Sicily in Italy, and from France and northern Portugal to northwest Turkey. It typically extends from 1000 to 1650 m a.s.l. (Jump et al., 2007). As *F. sylvatica* is parameterized both in the CCE region and in the ME region (CLRTAP, 2015), we divided its distribution area into these two regions based on Noirfalise (1987) and Rivas-Martinez (1995) climatic classifications (Fig. 1B).

Stomatal fluxes were calculated off-line by multiplying the hourly grid-averaged O_3 concentrations by the concurrent species-specific g_{sto}, and PODY was accumulated over the daylight hours of the growing season, as defined by CLRTAP (2015):

$$PODY = \sum_{i=1}^{N} max\left(g_{sto,i}\frac{r_{c,i}}{r_{b,i}+r_{c,i}}[O_3]_i - Y, 0\right)\Delta t \quad (2)$$

where N is the number of hours included in the calculation period, r_c is the total leaf surface resistance, r_b is the boundary-layer resistance, $[O_3]$ is ozone concentration and $\Delta t = 1$ h. The growing season was assumed to be year-long for Mediterranean species and last from April 1st to September 30th for temperate species (Table 2). As CHIMERE provides O_3 concentrations at a height of 20–25 m, we considered these to be representative of the top of a forest canopy and thus to provide a reasonable estimate of the concentration at the upper boundary of the laminar boundary layer adjacent to the upper canopy leaves, which is required for calculating PODY with Eq. (2) (CLRTAP, 2015). Even though CLRTAP (2015) suggests a lower height for some Mediterranean trees, we considered an average height of 20 m applicable for all the Mediterranean species included in our study, on the basis of Lemoine (1991), Condes and Sterba (2008), Gorgoso-Varela et al. (2015), and Hoshika et al. (in press).

The calculation of g_{sto} either included or excluded f_{SWC} so that both $PODY_{SWC+}$ and $PODY_{SWC-}$ were calculated, respectively. For each tree species, the PODY indices were calculated for four Y thresholds: 0, 1, 2 and 3 nmol m^{-2} s^{-1}.

2.3. Data from field measurements

There are very few Southern European forest sites where, at the same time, SWC and O_3 concentrations have been recorded over a long period of time. To test the results obtained from modelled data, we used measurements from the *Q. ilex* forest at Castelporziano (41.42 °N, 12.21 °E) in central Italy (Fig. 1), where semi-hourly air temperature and relative humidity (HC2S3 sensor, Campbell Scientific), 10-cm depth SWC (CS650 sensor, Campbell Scientific), solar radiation (Vantage Pro meteorological station, Davis Instruments) and O_3 concentrations (Model 49i analyzer, Thermo Scientific) were measured over the years 2013–2014. The forest is located at 13 m a.s.l. and 1.5 km from the seashore. The soil has a sandy texture and low water-holding capacity, which exacerbates drought. More details on soil and site characteristics are provided by Fares et al. (2013b, 2014). For the site-specific calculations, an empirical parameterization was used for g_{max} (204 mmol O_3 m^{-2} s^{-1}, Fares et al., 2013b) and f_{SWC} (FC = 0.250 m^3 m^{-3}, WP = 0.025 m^3 m^{-3}) (Fares, unpublished data). A validation of the POD modelled by DO3SE versus eddy-covariance measurements of stomatal ozone uptake at Castelporziano is provided by Hoshika et al. (in press).

2.4. Mapping and data analysis

For every tree species, maps of PODY averages, over two years

Table 1
Main characteristics of the 14,546 sites during the growing seasons of 2012 and 2013 (±SD). Each site corresponds to a 6 km × 6 km pixel in the coupled WRF-CHIMERE modelling system. The forest species occurrence in each pixel was determined by means of EUFORGEN vegetation maps. Data are from WRF-CHIMERE.

Dominant forest species	Climate	No of sites	Mean temperature (°C)	Total precipitation (mm)	Soil water content (%)
Abies alba	Temperate	2797	11.2 ± 3.2	517 ± 225	31.5 ± 8.1
Fagus sylvatica	Temperate/Mediterranean	4022	13.1 ± 2.5	406 ± 196	30.4 ± 7.2
Pinus cembra	Temperate	1546	6.2 ± 3.7	682 ± 238	35.1 ± 14.8
Pinus sylvestris	Temperate	3498	11.0 ± 4.0	524 ± 230	31.5 ± 14.8
Pinus halepensis	Mediterranean	530	13.1 ± 1.6	436 ± 167	32.1 ± 14.9
Pinus pinaster	Mediterranean	972	12.3 ± 2.2	496 ± 237	30.4 ± 10.1
Pinus pinea	Mediterranean	658	16.0 ± 1.2	396 ± 132	29.1 ± 9.0
Quercus suber	Mediterranean	523	14.3 ± 1.0	334 ± 113	30.8 ± 14.7

Table 2
Parameters used in the DO_3SE model (for equations see CLRTAP, 2015), where g_{max} is maximum stomatal conductance, a is light response constant, T_{opt}, T_{min} and T_{max} are the optimum, minimum and maximum temperature for stomatal conductance, VPD_{min} is the vapour pressure deficit limit for maximal stomatal effect, VPD_{max} is the lower VPD limit for stomatal limitation, f_{min} is fractional minimum stomatal conductance, and SGS and EGS denote the start and end of growing season. Data are from CLRTAP (2015).

Climate	Mediterranean			Temperate	
Parameterization	Mediterranean Europe			Continental central Europe	
Plant species	*Pinus halepensis*	*Fagus sylvatica*	*Quercus ilex*	*Picea abies*	*Fagus sylvatica*
g_{max} [mmol O_3 m^{-2} s^{-1}]	215	100	134	125	132
a [μmol^{-1} m^2 s]	0.013	0.006	0.012	0.010	0.006
T_{opt} [°C]	27	21	23	14	16
T_{min} [°C]	10	4	1	0	5
T_{max} [°C]	38	37	39	35	33
VPD_{min} [kPa]	3.2	4.0	4.0	3.0	3.1
VPD_{max} [kPa]	1.0	1.0	2.2	0.5	1.0
f_{min}	0.15	0.02	0.02	0.16	0.13
SGS	January 1st	April 1st	January 1st	April 1st	April 1st
EGS	December 31st	September 30th	December 31st	September 30th	September 30th

Table 3
WRF parameterization of wilting point (WP, m^3 m^{-3}) and field capacity (FC, m^3 m^{-3}) for estimating the soil water content function f_{SWC} for different soil types. Soil type was obtained from the LSM-Noah model (Chen and Dudhia, 2001).

Soil category	Soil type	Wilting point	Field capacity
1	Sand	0.010	0.339
2	Loamy Sand	0.028	0.421
3	Sandy Loam	0.047	0.434
4	Silt Loam	0.084	0.476
5	Silt	0.084	0.476
6	Loam	0.066	0.439
7	Sandy Clay Loam	0.067	0.404
8	Silty Clay Loam	0.120	0.464
9	Clay Loam	0.103	0.465
10	Sandy Clay	0.100	0.406
11	Silty Clay	0.126	0.468
12	Clay	0.138	0.468
13	Organic Material	0.066	0.439
14	Water	0	1
15	Bedrock	0.006	0.200
16	Other (land-ice)	0.028	0.421

(2012–2013) with and without SWC limitation, were created by a geographic information system (ARC-GIS 9.3, ESRI - Redlands, CA, USA) at a spatial resolution of 6 km × 6 km. At each site and Y threshold, the annual percent difference (Δ%) between $PODY_{SWC+}$ and $PODY_{SWC-}$ was calculated as:

$$\Delta\% = (PODY_{SWC-} - PODY_{SWC+})/PODY_{SWC+} \times 100 \quad (3)$$

This difference estimates the bias due to using the DO_3SE model without considering the soil water limitation to stomatal conductance.

3. Results

Fig. 2 summarizes the species-specific PODY averages, with and without f_{SWC}, for each of the four Y thresholds. The mean $POD0_{SWC+}$ ranged from 14 mmol m^{-2} for *F. sylvatica* to 29 mmol m^{-2} for *P. halepensis*, while the mean $POD0_{SWC-}$ ranged from 23 mmol m^{-2} for *F. sylvatica* to 57 mmol m^{-2} for *P. pinea*. *F. sylvatica* was the species with the lowest $POD1_{SWC-}$, $POD1_{SWC+}$, $POD2_{SWC-}$, $POD2_{SWC+}$ and $POD3_{SWC-}$, while *Q. suber* showed the lowest $POD3_{SWC+}$. *P. pinea* was the species with the highest $POD1_{SWC-}$, $POD2_{SWC-}$ and $POD3_{SWC-}$, while *P. pinaster* showed the highest $POD1_{SWC+}$, $POD2_{SWC+}$ and $POD3_{SWC+}$.

Our results show that the differences between $PODY_{SWC+}$ and $PODY_{SWC-}$ increased with increasing uptake thresholds (Fig. 3). Averaged over all species, Δ% increased by 78%, 128%, 237% and 565% for Y thresholds of 0, 1, 2 and 3 nmol O_3 m^{-2} s^{-1}, respectively. Fig. 3 lists the plant species along an increasing thermophile order, thus showing that Δ% was higher for Mediterranean vegetation (*P. pinaster* 89–356%, *P. halepensis* 96–429%, *P. pinea* 107–532%, *Q. suber* 103–1602%) than for temperate vegetation (*P. cembra* 50–340%, *P. sylvestris* 57–362%, *Abies alba* 57–371%) at any Y. A high Δ%, however, was also recorded for the temperate species *F. sylvatica* for POD3 (524%). This is explained by the fact that many $POD3_{SWC+}$ values were close to zero (5.5% of the values were <0.1 mmol m^{-2}), which amplified the difference Δ% between $POD3_{SWC+}$ and $POD3_{SWC-}$ (min. value = 1.4 mmol m^{-2}).

The spatial distribution of $PODY_{SWC-}$ markedly differed from the distribution of $PODY_{SWC+}$, as shown for POD0 in Fig. 4. The spatial discrepancies were higher among the Mediterranean species (e.g. *P. pinaster*) than the temperate species (e.g. *P. sylvestris*).

As an example of species, Fig. 5 shows the spatial distribution of Δ% for PODY values for different Y, calculated with and without the SWC function for a widely distributed species, i.e. *F. sylvatica*. The higher was the threshold Y, the higher became Δ%. Maps for all the species are presented in the supplementary material (Fig. 1S), confirming that the difference between $PODY_{SWC+}$ and $PODY_{SWC-}$ consistently increased with increasing Y values. In addition, the differences increased from the North to the South and were higher for Mediterranean than for temperate species.

The results obtained from the PODY calculations that were based on the meteorological and ozone measurements in a *Q. ilex* forest and the local parameterization were in broad agreement with those obtained from the model calculations (Fig. 6). Also in this case, the expected dependence on Y was evident: the higher the threshold Y, the higher the difference between $PODY_{SWC+}$ and $PODY_{SWC-}$(Fig. 6A and B). The average Δ% for *Q. ilex* over the two years ranged from 472 to 1037% depending on Y (Fig. 6C). The difference Δ% was higher for the measurement-based PODY than for the modelled PODY, largely due to an overestimation of the modelled SWC values, which resulted in weaker stomatal limitations, even if considering the differences in the g_{sto} parameterization (Fig. 7).

4. Discussion

Risk assessment of O_3 effects on vegetation is gradually moving from concentration-based exposure metrics to a more physiologically based approach that requires modelling of stomatal O_3 flux to plants (Tuovinen et al., 2009; CLRTAP, 2015). Identifying major research needs for DO_3SE, Tuovinen et al. (2009) suggested that the incorporation of SWC effects is the most urgent of these needs, even though the determination of soil moisture and the related stomatal response functions has been shown to be challenging

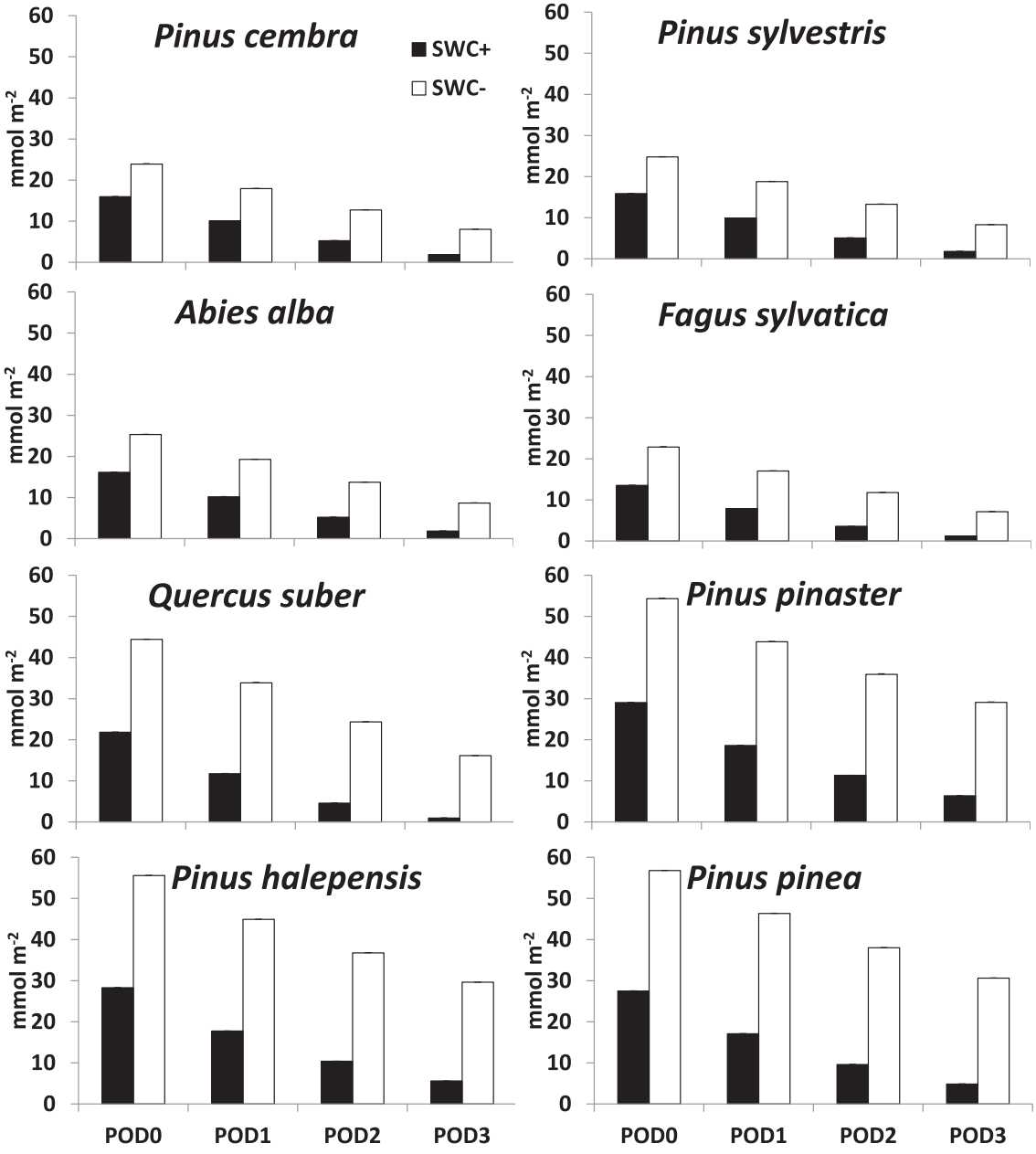

Fig. 2. Phytotoxic Ozone Dose (POD*Y*) calculated with four *Y* thresholds of O_3 uptake (0, 1, 2 and 3 nmol O_3 m^{-2} s^{-1}), with (SWC+) and without (SWC−) the soil water content limitation to stomatal O_3 uptake. Values are averages over two years (2012–2013) of the 6 km × 6 km pixels where the species was dominant (according to EUFORGEN vegetation maps).

(Emberson et al., 2007). Indeed, a soil moisture module was subsequently developed and incorporated in DO_3SE (Büker et al., 2012). However, this kind of site-specific model requires extensive input data that may not be easily available. As SWC does not represent an important limiting factor to stomatal aperture in all climates (e.g. Hoshika et al., 2013), in some cases such a limitation can be realistically neglected to simplify POD*Y* modelling; i.e. $f_{SWC} = 1$ can be set in Eq. (1). However, this may not be justified for water-limited ecosystems where soil water availability plays a major role in photosynthetic limitations (Keenan et al., 2010). It is worth noting that dry and semi-dry habitats cover about 41% of Earth's land surface (Reynolds et al., 2007) and that future projections foresee a drier climate in Southern Europe (IPCC, 2014), where drought conditions occur frequently in drylands and water-limited environments.

The data required for estimating soil moisture range from those which are often readily available from standard meteorological observations, such as precipitation and temperature, to data which are typically recorded only at selected research sites, such as soil characteristics, root distribution and water fluxes (Tuovinen et al., 2009). However, for a large-scale epidemiological assessment of O_3 risk to vegetation, estimation of such data can be achieved from modern weather modelling systems, such as the WRF-CHIMERE system, that can simulate large-scale SWC data at fine spatial resolution and with reasonably good accuracy (Anav et al., 2016).

By using modelled input data for Southern European forest sites, we demonstrated that the differences between POD*Y* values calculated with and without SWC limitation were significant. As expected, calculating POD*Y* without the SWC limitation produced higher values than with that limitation included. This is the first

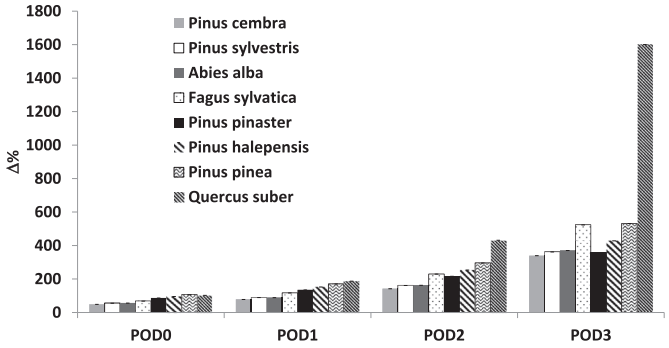

Fig. 3. Average percent difference (Δ%) in POD*Y* due to ignoring the soil water content limitation to stomatal O_3 uptake. Species are sorted along an increasing thermophile order.

work that quantifies such differences in a regional-scale application. In agreement with the finding that soil water deficit is a frequent phenomenon in Mediterranean climates (Paoletti, 2006), the differences between POD*Y* values calculated with and without f_{SWC} increased from the temperate climate in the North to the Mediterranean climate in the South, and from the temperate to Mediterranean species.

A comparison of modelled and measured SWC data at an individual *Q. ilex* site showed that WRF-CHIMERE was able to simulate well the seasonal SWC distribution, but the modelled values were systematically higher than the measured ones (on average by 0.15 $m^3\ m^{-3}$). Such a model overestimation made the difference Δ% lower than when using measured (lower) SWC data. Similarly, the positive bias in the modelled O_3 concentration, typical for WRF-CHIMERE simulations (Anav et al., 2016), implies a lower difference Δ% for $Y > 0$ than when using measured (lower) O_3 data. These reductions of Δ% result from the definition of POD*Y* that cuts out a constant threshold flux (Eq. (2)), which has a larger relative effect on the smaller fluxes. Anyhow, the measurement-based results confirm our two main results, i.e. that calculating POD*Y* without f_{SWC} causes a significant difference, and that this difference strongly increases with increasing *Y* threshold.

It should be noted that the WRF-CHIMERE simulations represent large-scale distributions, so site-specific differences are to be expected. If the overestimation of SWC occurs across the model domain, the magnitude of differences in estimating POD*Y* without the SWC function will be higher under real-world conditions than what our modelled SWC data suggest. It is worth noting that we used SWC data for the top 10 cm of soil, which maximized the difference between $POD Y_{swc+}$ and $POD Y_{swc-}$. However, the effect of stomatal limitation due to SWC was very strong even when POD*Y* was calculated with the SWC measured in deeper layer (Table 1S). Anyhow, our approach represents a worst-case scenario, as the uppermost soil layers are expected to dry out more easily than deeper layers. Most of the absorbing fine roots, however, concentrate in the top soil layer and only a minimal fraction reaches depths below 50 cm (Jackson et al., 1996; Vinceti et al., 1998). Some species may send a few roots very deep in the soil, e.g. 13 m on average for Mediterranean trees (Canadell et al., 1996), although the functional significance of such deep roots is not well understood yet. A major role seems to be the 'hydraulic lift', i.e. at night deep roots of large trees take up water from the deep soil layer and shallow roots release water back to the upper soil layers (Filella and Penuelas, 2004).

Overall, these results suggest that the SWC function has to be incorporated into the simulation of POD*Y* carried out under water-limited conditions because (i) the differences resulting from the assumption $f_{SWC} = 1$ are very significant and higher for the Mediterranean species, and (ii) the spatial distribution of $POD Y_{swc-}$

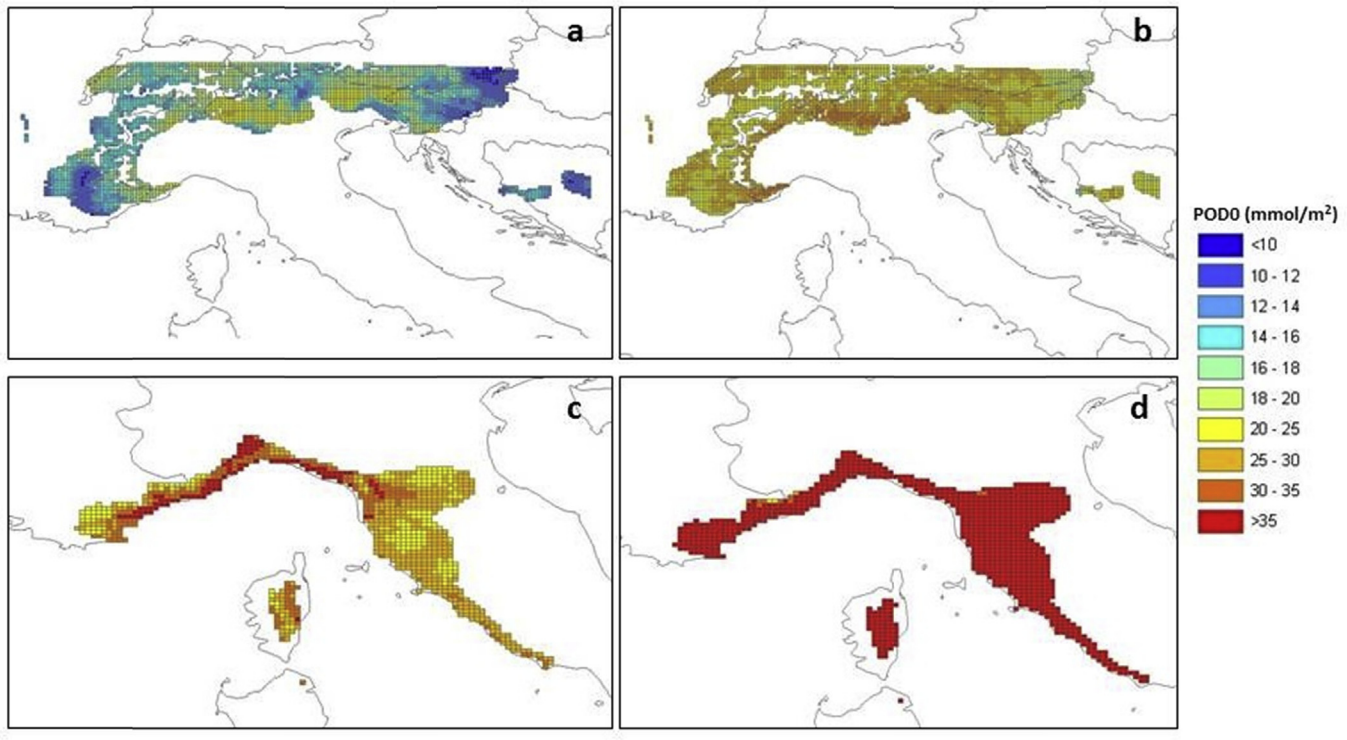

Fig. 4. Spatial distribution of annual $POD0_{swc+}$ (a, c) and $POD0_{swc-}$ (b, d) for one temperate species (*P. sylvestris*, top) and one Mediterranean species (*Pinus pinaster*, bottom). Values are averages over two years (2012–2013) of the 6 km × 6 km pixels where the species was dominant (according to EUFORGEN vegetation maps).

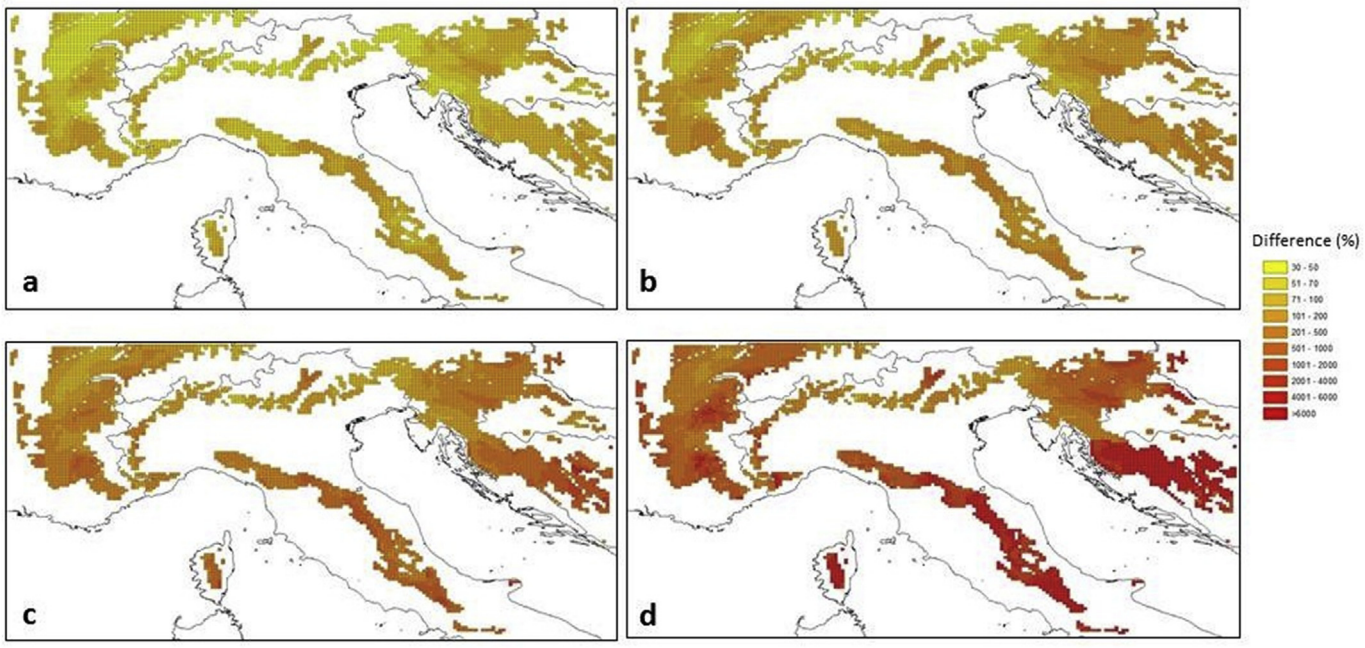

Fig. 5. Spatial distribution of percent difference (Δ%) of annual POD0 (a), POD1 (b), POD2 (c) and POD3 (d) due to ignoring the soil water content function in the DO_3SE model for *Fagus sylvatica*. Values are averages over two years (2012–2013) of the 6 km × 6 km pixels where the species was dominant (according to EUFORGEN vegetation maps).

markedly differs from that of POD_{SWC}. Although larger Δ% values were found for Mediterranean than temperate species, also the latter exhibited large differences when f_{SWC} was not included in the model. This result suggests that the importance of SWC effect should be considered in any POD*Y* simulation, not only in severely water-limited environments.

Our results are consistent with the observation that the sensitivity of POD*Y* to the inputs typically increases with the value of the threshold (Tuovinen et al., 2007; Klingberg et al., 2008). Indeed, it has been shown that this is a universal property of mathematical functions of this kind (Sofiev and Tuovinen, 2001). The threshold *Y* is intended to incorporate the plant ability to detoxify O_3 and maintain reactive oxygen species below a toxic threshold (Mills et al., 2011b). Threshold-based indices in general assume that plants have adapted to low, pre-industrial, naturally occurring O_3 levels and thus discard values below a corresponding threshold of O_3 uptake or concentration (Paoletti and Manning, 2007). *Y* can also be viewed as a parameter of a statistical index, so the value of this parameter can be determined by optimizing the relationship between POD*Y* and the observed vegetation response. We tested four plausible thresholds: $Y = 0$ nmol O_3 m^{-2} s^{-1} as suggested by the assumption that any O_3 molecule entering into a leaf may induce a metabolic response (Musselman et al., 2006), 1 nmol m^{-2} s^{-1} as recommended by CLRTAP (2015) for forest trees, 2 nmol m^{-2} s^{-1} that is under discussion for a new threshold for forests (Büker et al., 2015), and 3 nmol m^{-2} s^{-1} to further illustrate the sensitivity of POD*Y* to *Y*. Our results indicate that, from a sensitivity point of view, the threshold *Y* should be kept as low as possible.

A critical level, i.e. the cumulative stomatal flux above which direct adverse effects on sensitive vegetation may occur according to present knowledge, has been proposed in terms of POD1 for deciduous broadleaf forests (beech and birch, 4 mmol m^{-2}) and coniferous forests (Norway spruce, 8 mmol m^{-2}), based on data from temperate and boreal forests (CLRTAP, 2015). In this study, the average $POD1_{SWC+}$ values ranged from 7.8 mmol m^{-2} for the deciduous temperate/Mediterranean broadleaf *F. sylvatica* to 18.6 mmol m^{-2} for the Mediterranean conifer *P. pinaster*. Even the field measurements, where low SWC values limited stomatal uptake, resulted in a value of 7.1 mmol m^{-2} for the Mediterranean evergreen broadleaf *Q. ilex*. Ignoring the SWC limitation to stomatal uptake would result in a serious overestimation of critical level exceedances and thus overstate the ozone-induced risks to vegetation. A future development may be the use of process-based models that link O_3 uptake with carbon assimilation through the Ball-Berry parameterization (Ball et al., 1987), as demonstrated by Anav et al. (2012) and Hoshika et al. (in press).

5. Conclusions

Flux-based risk assessment of O_3 effects on vegetation is gradually superseding the exposure-based assessment. Ideally, O_3 risk assessment maps should be generated from measurements of stomatal O_3 flux (Tuovinen et al., 2009). However, data sets suitable for this are scarce (e.g. Tuovinen et al., 2004, 2007; Fares et al., 2013b) and thus the regional-scale assessment of O_3 risk to vegetation is dependent on modelling. By using the DO_3SE flux model and modelled input data for 14,546 grid-based Southern European forest sites distributed in temperate and Mediterranean climates, we demonstrated that the differences between the accumulated stomatal O_3 flux (POD*Y*) values calculated either with or without SWC limitation (i) were significant, (ii) strongly increased with increasing flux thresholds, and (iii) increased from temperate to Mediterranean vegetation/climate. The quantification of these differences depends on the accuracy of the stomatal conductance model and of the meteorological/hydrological model used for producing the SWC and other input for the stomatal model. As the soil moisture model employed here overestimated SWC relative to the measurements at an Italian forest site, the magnitude of differences can be higher under real-world conditions than what our model results suggest. We therefore recommend to (i) include the soil water content (f_{SWC}) function in any POD*Y* simulation, in order to avoid significant overestimation of O_3 risk to vegetation, in particular in water-limited environments, as the differences were higher for Mediterranean vegetation than for temperate

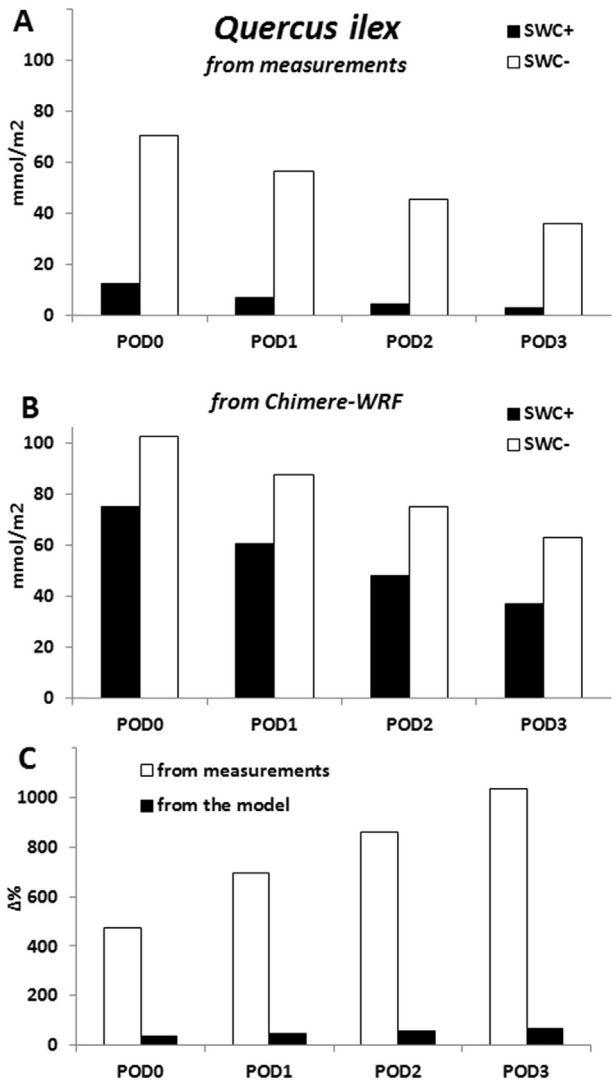

Fig. 6. Phytotoxic Ozone Dose (POD*Y*) values calculated with four *Y* thresholds of O_3 uptake flux (0, 1, 2 and 3 nmol O_3 m^{-2} s^{-1}), with (SWC+) and without (SWC$^-$) the soil water content limitation in 2013 at the *Quercus ilex* forest of Castelporziano. The values were calculated on the basis of field measurements and empirical parameterization (A) and modelled data and CLRTAP (2015) parameterization (B). Percent differences are shown in C.

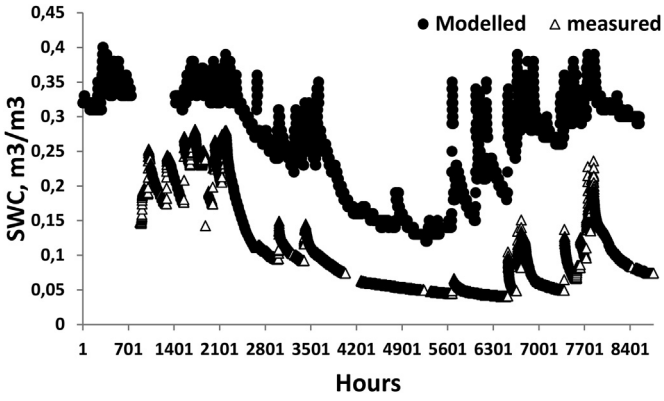

Fig. 7. Measured and modelled hourly soil water content (SWC, 10 cm depth) at a *Quercus ilex* forest (Castelporziano) in central Italy in 2013.

vegetation; and (ii) use the a low *Y* threshold in O_3 risk assessment due to the increasing sensitivity of POD*Y* to inputs with increasing *Y*.

Appendix A. Supplementary data

Supplementary data related to this article can be found at http://dx.doi.org/10.1016/j.atmosenv.2016.09.066.

References

Alonso, R., Elvira, S., Sanz, M.J., Gerosa, G., Emberson, L.D., Bermejo, V., Gimeno, B.J., 2008. Sensitivity analysis of a parameterization of the stomatal component of the DO3SE model for Quercus ilex to estimate ozone fluxes. Environ. Pollut. 155, 473–480.

Anav, A., Menut, L., Khvorostyanov, D., Viovy, N., 2012. A comparison of two canopy conductance parameterizations to quantify the interactions between surface ozone and vegetation over Europe. J. Geophys. Res. 117, G03027.

Anav, A., De Marco, A., Proietti, C., Alessandri, A., Khvorostyanov, D., Menut, L., Paoletti, E., Sicard, P., Sitch, S., Vitale, M., 2016. Comparing concentration-based (AOT40) and stomatal uptake (PODY) metrics for ozone risk assessment to European forests. Glob. Change Biol. 22, 1608–1627.

Ball, J.T, Woodrow, I.E., Berry, J.A., 1987. A model predicting stomatal conductance and its contribution to the control of photosynthesis under different environmental conditions. In: Biggens, J. (Ed.), Progress in Photosynthesis Research. Martinus Nijhoff Publishers, The Netherlands.

Bessagnet, B., Hodzic, A., Vautard, R., Beekmann, M., Cheinet, S., Honoré, C., Liousse, C., Rouil, L., 2004. Aerosol modelling with CHIMERE - preliminary evaluation at the continental scale. Atmos. Environ. 38, 2803–2817.

Büker, P., Emberson, L.D., Ashmore, M.R., Cambridge, H.M., Jacobs, C.M.J., Massman, W.J., Müller, J., Nikolov, N., Novak, K., Oksanen, E., Schaub, M., de la Torre, D., 2007. Comparison of different stomatal conductance algorithms for ozone flux modelling. Environ. Pollut. 146, 726–735.

Büker, P., Morrissey, T., Briolat, A., Falk, R., Simpson, D., Tuovinen, J.-P., Alonso, R., Barth, S., Baumgarten, M., Grulke, N., Karlsson, P.E., King, J., Lagergren, F., Matyssek, R., Nunn, A., Ogaya, R., Peñuelas, J., Rhea, L., Schaub, M., Uddling, J., Werner, W., Emberson, L.D., 2012. DO_3SE modelling of soil moisture to determine ozone effects to forest trees. Atmos. Chem. Phys. 12, 5537–5562.

Büker, P., Feng, Z., Uddling, J., Briolat, A., Alonso, R., Braun, S., Elvira, S., Gerosa, G., Karlsson, P.-E., Le Thiec, D., Marzuoli, R., Mills, G., Oksanen, E., Wieser, G., Wilkinson, M., Emberson, L., 2015. New flux based dose-response relationships for ozone for European forest tree species. Environ. Pollut 206, 163–174.

Butkovic, V., Cvitas, T., Klasing, L., 1990. Photochemical ozone in the mediterranean. Sci. Total Environ. 99, 145–151.

Canadell, J., Jackson, R.B., Ehleringer, J.R., Mooney, H.A., Sala, O.E., Schulze, E.-D., 1996. Maximum rooting depth of vegetation types at the global scale. Oecologia 108, 583–595.

Ceppi, A., Ravazzani, G., Corbari, C., Salerno, R., Meucci, S., Mancini, M., 2013. Real time drought forecasting system for irrigation management. Hydrol. Earth Syst. Sci. Discuss. 10, 15811–15840.

Chen, F., Dudhia, J., 2001. Coupling an advanced land surface–hydrology model with the Penn state–NCAR MM5 modeling system - Part I: model implementation and sensitivity. Mon. Weather Rev. 129, 569–585.

Chen, F., Manning, K.W., Lemone, M., Trier, S.B., Alfieri, J.G., Roberts, R., Tewari, M., Niyogi, D., Horst, T.W., Oncley, S.P., Basara, J.B., Blanken, P.D., 2007. Description and evaluation of the characteristics of the NCAR high-resolution land data assimilation system. J. Appl. meteorol. Climatol. 46, 694–713.

CLRTAP, 2015. Manual on Methodologies and Criteria for Modelling and Mapping Critical Loads and Levels and Air Pollution Effects, Risks and Trends. Chapter 3: Mapping Critical Levels for Vegetation. United Nations Economic Commission for Europe (UNECE), Geneva, p. 254. Convention on Long-range Transboundary Air Pollution.

Condes, S., Sterba, H., 2008. Comparing an individual tree growth model for Pinus halepensis Mill. in the Spanish region of Murcia with yield tables gained from the same area. Eur. J. For. Res. 127, 253–261.

De Meij, A., Gzella, A., Cuvelier, C., Thunis, P., Bessagnet, B., Vinuesa, J.F., Menut, L., Kelder, H., 2009. The impact of MM5 and WRF meteorology over complex terrain on CHIMERE model calculations. Atmos. Chem. Phys. 9, 6611–6632.

Di Matteo, G.D., Perini, L., Atzori, P., De Angelis, P., Mei, T., Bertini, G., Fabbio, G., Scarascia-Mugnozza, G., 2014. Changes in foliar carbon isotope composition and seasonal stomatal conductance reveal adaptive traits in Mediterranean coppices affected by drought. J. For. Res. 25, 839.

EEA, 2013. Air Quality in Europe- 2013 Report. European Environment Agency Report No 9/2013, p. 107. http://dx.doi.org/10.2800/92843. ISBN 978-92-9213-406-8.

Emberson, L., Ashmore, M.R., Cambridge, H.M., Simpson, D., Tuovinen, J.-P., 2000. Modelling stomatal ozone flux across Europe. Environ. Pollut. 109, 403–413.

Emberson, L., Ashmore, M., Simpson, D., Tuovinen, J.-P., Cambridge, H., 2001. Modelling and mapping ozone deposition in Europe. Water, Air Soil Pollut. 130, 577–582.

Emberson, L.D., Büker, P., Ashmore, M.R., 2007. Assessing the risk caused by ground level ozone to European forests: a case study in pine, beech and oak across different climate regions. Environ. Pollut. 147, 454–466.

Fares, S., Vargas, R., Detto, M., Goldstein, A.H., Karlik, J., Paoletti, E., Vitale, M., 2013a. Tropospheric ozone reduces carbon assimilation in trees: estimates from analysis of continuous flux measurements. Glob. Change Biol. 19, 2427–2443.
Fares, S., Matteucci, G., Scarascia Mugnozza, G., Morani, A., Calfapietra, C., Salvatori, E., Fusaro, L., Manes, F., Loreto, F., 2013b. Testing of models of stomatal ozone fluxes with field measurements in a mixed Mediterranean forest. Atmos. Environ. 67, 242–251.
Fares, S., Savi, F., Muller, J., Matteucci, G., Paoletti, E., 2014. Simultaneous measurements of above and below canopy ozone fluxes help partitioning ozone deposition between its various sinks in a Mediterranean Oak forest. Agric. For. Meteorol. 198–199, 181–191.
Filella, I., Penuelas, J., 2004. Indications of hydraulic lift by Pinus halepensis and its effects on the water relations of neighbour shrubs. Biol. Plant. 47, 209–214.
Fiore, A.M., Jacob, D.J., Field, B.D., Streets, D.G., Fernandes, S.D., Jang, C., 2002. Linking ozone pollution and climate change: the case for controlling methane. Geophys. Res. Lett. 29, 1919.
Gorgoso-Varela, J.J., García-Villabrille, J.D., Rojo-Alboreca, A., 2015. Modeling extreme values for height distributions in Pinus pinaster, Pinus radiata and Eucalyptus globulus stands in northwestern Spain. iForest 9, 23–29.
Günthardt-Goerg, M.S., Vollenweider, P., 2007. Linking stress with macroscopic and microscopic leaf response in trees: new diagnostic perspectives. Environ. Pollut. 147, 467–488.
Greve, P., Warrach-Sagi, K., Wulfmeyer, V., 2013. Evaluating soil water content in a WRF-Noah downscaling experiment. J. Appl. meteorol. 52, 2313–2327.
Hoshika, Y., Pecori, F., Conese, I., Bardelli, T., Marchi, E., Manning, W.J., Badea, O., Paoletti, E., 2013. Effects of a three-year exposure to ambient ozone on biomass allocation in poplar using ethylenediurea. Environ. Pollut. 180, 299–303.
Hoshika, Y., Fares, S., Savi, F., Gruening, C., Goded, I., De Marco, A., Sicard, P., Paoletti, E., 2016. Stomatal conductance models for ozone risk assessment at canopy level in two Mediterranean evergreen forests. Agric. For. Meteorol. in press.
Climate Change 2014 Intergovernmental Panel on Climate Change, 2014. Impacts, Adaptation, and Vulnerability: Contribution of Working Group II to the Fifth Assessment Report of the Intergovernmental Panel on Climate Change.
Jackson, R.B., Canadell, J., Ehleringer, J.R., Mooney, H.A., Sala, O.E., Schulze, E.D., 1996. A global analysis of root distribution for terrestrial biomes. Oecologia 108, 389–411.
Jarvis, P.G., 1976. The interpretation of the variations in leaf water potential and stomatal conductance found in canopies in the field. R. Soc. Publ. 273, 593–610.
Jump, A., Hunt, J., Penuelas, J., 2007. Climate relationships of growth and establishment across the altitudinal range of Fagus sylvatica in the Montseny Mountains, northeast Spain. Ecoscience 14, 507–518.
Keenan, T., Sabate, S., Gracia, C., 2010. Soil water stress and coupled photosynthesis–conductance models: bridging the gap between conflicting reports on the relative roles of stomatal, mesophyll conductance and biochemical limitations to photosynthesis. Agric. For. Meteorol. 150, 443–453.
Kim, H.C., Nga, F., 2011. Improvement of Meteorological Modeling by Accurate Prediction of Soil Moisture in the Weather Research and Forecasting Model. Final report. Air Resources Laboratory National Oceanic and Atmospheric Administration. U.S. Dep. Commer. March 31, 2011.
Klingberg, J., Danielsson, H., Simpson, D., Pleijel, H., 2008. Comparison of modelled and measured ozone concentrations and meteorology for a site in south-west Sweden: implications for ozone uptake calculations. Environ. Pollut. 155, 99–111.
Lemoine, B., 1991. Growth and yield of maritime pine (Pinus pinaster Ait): the average dominant tree of the stand. Ann. Des. Sci. For. 48 (5), 593–611. INRA/EDP Sciences.
Llusia, J., Roahtyn, S., Yakir, D., Rotenberg, E., Seco, R., Guenther, A., Penuelas, J., 2016. Photosynthesis, stomatal conductance and terpene emission response to water availability in dry and mesic Mediterranean forests. Trees 30, 749.
Mills, G., Hayes, F., Simpson, D., Emberson, L., Norris, D., Harmens, H., Büker, P., 2011a. Evidence of widespread effects of ozone on crops and (semi-)natural vegetation in Europe (1990-2006) in relation to AOT40- and flux-based risk maps. Glob. Change Biol. 17, 592–613.
Mills, G., Pleijel, H., Braun, S., Büker, P., Bermejo, V., Calvo, E., Danielsson, H., Emberson, L., González Fernández, I., Grünhage, L., Harmens, H., Hayes, F., Karlsson, P.-E., Simpson, D., 2011b. New stomatal flux-based critical levels for ozone effects on vegetation. Atmos. Environ. 45, 5064–5068.
Musselman, R.C., Lefohn, A., Massman, W.J., Heath, R., 2006. A critical review and analysis of the use of exposure- and flux-based ozone indices for predicting vegetation effects. Atmos. Environ. 40, 1869–1888.
Noirfalise, A., 1987. Map of the Natural Vegetation of the Member Countries of the European Community and the Council of Europe. Council of Europe, CEC.
Paoletti, E., De Marco, A., Beddows, D.C.S., Harrison, R.M., Manning, W.J., 2014. Ozone levels in European and USA cities are increasing more than at rural sites, while peak values are decreasing. Environ. Pollut. 192, 295–299.
Paoletti, E., Ferrara, A.M., Calatayud, V., Cerveró, J., Giannetti, F., Sanz, M.J., Manning, W.J., 2009a. Deciduous shrubs for ozone bioindication: *Hibiscus syriacus* as an example. Environ. Pollut. 157, 865–870.
Paoletti, E., Contran, N., Bernasconi, P., Günthardt-Goerg, M.S., Vollenweider, P., 2009b. Structural and physiological responses to ozone in Manna ash (*Fraxinus ornus* L.) leaves in seedlings and mature trees under controlled and ambient conditions. Sci. Total Environ. 407, 1631–1643.
Paoletti, E., 2007. Ozone impacts on forests. Cab reviews: perspectives in agriculture, veterinary science. Nutr. Nat. Resour. 2 (68), 13 n° 068.
Paoletti, E., Manning, W.J., 2007. Toward a biologically significant and usable standard for ozone that will also protect plants. Environ. Pollut. 150, 85–95.
Paoletti, E., 2006. Impact of ozone on Mediterranean forests: a review. Environ. Pollut. 144, 463–474.
Reynolds, J.F., Stafford Smith, D.M., Lambin, E.F., Turner II, B.L., Mortimore, M., Batterbury, S.P., Downing, T.E., Dowlatabadi, H., Fernandéz, R.J., Herrick, J.E., Huber-Sannwald, E., Jiang, H., Leemans, R., Lynam, T., Maestre, F.T., Ayarza, M., Walker, B., 2007. Global desertification: building a science for dryland development. Science 316, 847–851.
Rivas-Martinez, S., 1995. Bases para una nueva clasificacion bioclimatica de la Tierra. Folia Bot. Matr. 16.
Sicard, P., Serra, R., Rossello, P., 2016a. Spatiotemporal trends of surface ozone concentrations and metrics in France. Environ. Res. 149, 122–144.
Sicard, P., De Marco, A., Dalstein-Richier, L., Tagliaferro, F., Paoletti, E., 2016b. An epidemiological assessment of stomatal ozone flux-based critical levels for visible ozone injury in Southern European forests. Sci. Total Environ. 541, 729–741.
Sicard, P., De Marco, A., Troussier, F., Renou, C., Vas, N., Paoletti, E., 2013. Decrease in surface ozone concentrations at Mediterranean remote sites and increase in the cities. Atmos. Environ. 79, 705–715.
Sicard, P., Thibaudon, M., Besancenot, J.-P., Mangin, A., 2012. Forecast models and trends for the main characteristics of the Olea pollen season in Nice (south-eastern France) over the 1990-2009 period. Grana 51, 52–62.
Sicard, P., Vas, N., Calatayud, V., García-Breijo, F.J., Reig-Armiñana, J., Sanz, M.J., Dalstein-Richier, L., 2010. Dommages forestiers et pollution à l'ozone dans les réserves naturelles : le cas de l'arolle dans le sud-est de la France. Forêt Méditerr. XXXI 273–286.
Sicard, P., Coddeville, P., Galloo, J.C., 2009. Near-surface ozone levels and trends at rural stations in France over the 1995-2003 period. Environ. Monit. Assess. 156, 141–157.
Simpson, D., Ashmore, M., Emberson, L., Tuovinen, J.-P., 2007. A comparison of two different approaches for mapping potential ozone damage to vegetation. A model study. Environ. Pollut. 146, 715–725.
Simpson, D., Benedictow, A., Berge, H., Bergström, R., Emberson, L.D., Fagerli, H., Flechard, C.R., Hayman, G.D., Gauss, M., Jonson, J.E., Jenkin, M.W., Nyíri, A, Richter, C., Semeena, V.S, Tsyro, S., Tuovinen, J.-P., Valdebenito, A., Wind, P., 2012. The EMEP MSC-W chemical transport model technical description. Atm. Chem. Phys. 12, 7825–7865.
Skamarock, W.C., Klemp, J.B., Dudhia, J., Gill, D.O., Baker, D.M., Duda, M.G., Huang, X.-Y., Wang, W., Powers, J.G., 2008. A Description of the Advanced Research WRF Version 3, NCAR Tech. Note NCAR/TN-475/STR, p. 113.
Sofiev, M., Tuovinen, J.-P., 2001. Factors determining the robustness of AOT40 and other ozone exposure indices. Atmos. Environ. 35, 3521–3528.
Tuovinen, J.-P., Emberson, L., Simpson, D., 2009. Modelling ozone fluxes to forests for risk assessment: status and prospects. Ann. For. Sci. 66, 401–414.
Tuovinen, J.-P., Simpson, D., Emberson, L., Ashmore, M., Gerosa, G., 2007. Robustness of modelled ozone exposures and doses. Environ. Pollut. 146, 578–586.
Tuovinen, J.-P., Ashmore, M., Emberson, L., Simpson, D., 2004. Testing and improving the EMEP ozone deposition module. Atmos. Environ. 38, 2373–2385.
Tuovinen, J.-P., Simpson, D., Mikkelsen, T.N., Emberson, L.D., Ashmore, M.R., Aurela, M., Cambridge, H.M., Hovmand, M.F., Jensen, N.O., Laurila, T., Pilegaard, K., Ro-Poulsen, H., 2001. Comparisons of measured and modelled ozone deposition to forests in Northern Europe. Water Air Soil Pollut. Focus 1, 263–274.
Vinceti, B., Paoletti, E., Wolf, U., 1998. Analysis of soil, roots and mycorrhizae in a Norway spruce declining forest. Chemosphere 36, 937–942.
Vingarzan, R., 2004. A review of surface O_3 background levels and trends. Atmos. Environ. 38, 3431–3442.
Wittig, V.E., Ainsworth, E.A., Naidu, S.L., Karnosky, D.F., Long, S.P., 2009. Quantifying the impact of current and future tropospheric ozone on tree biomass, growth, physiology and biochemistry: a quantitative meta-analysis. Glob. Change Biol. 15, 396–424.

Further reading

Elvira, S., Alonso, R., Gimeno, B.S., 2007. Simulation of stomatal conductance for Aleppo pine to estimate its ozone uptake. Environ. Pollut. 146, 617–623.
Nunn, A.J., Kozovits, A.R., Reiter, I.M., Heerdt, C., Leuchner, M., Lütz, C., Liu, X., Löw, M., Winkler, J.B., Grams, T.E.E., Häberle, K.-H., Werner, H., Fabian, P., Rennenberg, H., Matyssek, R., 2005. Comparison of ozone uptake and sensitivity between a phytotron study with young beech and a field experiment with adult beech (*Fagus sylvatica*). Environ. Pollut. 137, 494–506.
Paoletti, E., Nali, C., Lorenzini, G., 2007. Early responses to acute ozone in two *Fagus sylvatica* clones differing in xeromorphic adaptations: photosynthetic and stomatal processes, membrane and epicuticular characteristics. Environ. Monit. Assess. 128, 93–108.